doi:10.14311/ppt.2017.1.40
*Plasma Physics and Technology* **4**(1):40–43, 2017


# CALCULATION OF ARC POWER LOSSES IN THE SIMPLIFIED MODEL OF INTENSIVELY BLASTED ELECTRIC ARC

J. Senk*, I. Laznickova, I. Jakubova

*Faculty of Electrical Engineering and Communication, Brno University of Technology, Technická 12, 616 00 Brno, Czech Republic*

* senk@feec.vutbr.cz

**Abstract.** In previous versions of the simplified model of intensively blasted electric arc burning in argon in the arc heater's anode channel, the authors used the constant total power loss coefficient for estimation of arc power losses in all anode channel individual parts. Using this approach, the model with relatively low computational complexity has led to very good agreement between the total computed and experimentally obtained values, but when the computed and measured power losses of individual anode channel segments have been compared, considerable differences have been revealed. In the modified model, theoretically computed net emission coefficient of argon is used in the energy equation to express the arc power losses. This way, satisfactory accordance is achieved between not only the total, but also partial measured and computed values. Exemplary results are given in figures and tables and discussed.

**Keywords:** electric arc, model, experiment, power loss, net emission coefficient.

## 1. Introduction

The simplified model of intensively blasted electric arc burning in a cylindrical anode channel of the arc heater has been formulated [1] to be used for evaluating measured data and for getting an idea of the arc's behavior inside the experimental device. A modular-type arc heater has been designed [2] to investigate both its technological applications (e.g. for decomposition of stable harmful compounds) and its operational characteristics including also basic parameters of the arc inside, or the plasma jet at the output. Rather extent experience has been collected in the field of the design and operation, as well as in the field of modelling. Although the basics of the model remain unchanged, some presumptions or procedures have been modified in accordance with the results of numerous experiments and their analyses, and new versions of the model are created [3].

## 2. Estimation of the arc power loss using net emission coefficient

As described in details in [3], in previous versions of the arc model, only the (relative) differences of the measured and computed values of the total voltage and the total power loss of the arc have been evaluated as a condition for termination of the computation. Although such an approach is completely sufficient for estimation of output parameters, substantial deviations have been revealed between the measured and computed power losses of the arc in individual sections of the segmented anode channel. In other words, obviously the previous version of the model is not able to express power loss of the electric arc truly in all the parts of the arc heater's anode channel [3].

To explain this phenomenon, a short description of the used arrangement of the experimental device is useful. The arc heater consists of several separately cooled and electrically and thermally insulated parts, namely of the cathode (subscript $_{\mathrm{cat}}$), the input part of the anode channel including the cathode shell (subscript $_{\mathrm{in}}$), the main part of the anode channel (subscript $_{\mathrm{ch}}$), and the grounded part of the anode channel (the anode itself, subscript $_{\mathrm{an}}$). The arc power loss $P_{\mathrm{loss\_xx}}$ in each of these parts is determined separately. The electric arc (subscript $_{\mathrm{A}}$) is burning between the cathode tip (the arc beginning at the axial coordinate $z = 0$) and the end of the anode ($z = z_{\mathrm{L}}$) inside the cylindrical anode channel.

In the older version of the model the calculation was stopped in the $i$th step if the minimum of the following function was reached

$$
{}^{i}\delta_{\mathrm{tot0}} = \left\{ \left[ 1 - \frac{{}^{i}U_{\mathrm{A\_c}}(z_{\mathrm{L}}) I_{\mathrm{m}} + P_{\mathrm{loss\_cat\_m}} + {}^{i}P_{\mathrm{loss\_as\_c}}}{U_{\mathrm{m}} I_{\mathrm{m}}} \right]^2 + \left[ 1 - \frac{{}^{i}P_{\mathrm{loss\_tot\_c}}}{P_{\mathrm{loss\_tot\_m}}} \right]^2 \right\}^{\frac{1}{2}} \quad (1)
$$

Here, subscript $_{\mathrm{m}}$ stands for measured, $_{\mathrm{c}}$ for calculated, $_{\mathrm{tot}}$ for total, subscript $_{\mathrm{as}}$ means anode spot, superscript $^{i}$ indicates the number of the computational cycle.

As described in [3], the model has been modified to be able to evaluate the power losses of the individual parts of the anode channel (input, channel, and anode) separately, because these power losses are measured separately and thus, more detailed insight on the

behavior of the arc could be obtained. Related to this modification, also the objective function has been changed to the following

$$
{}^{i}\delta_{\mathrm{tot1}} = \left\{ \left[ 1 - \frac{{}^{i}U_{\mathrm{A\_c}}(z_{\mathrm{L}})I_{\mathrm{m}} + P_{\mathrm{loss\_cat\_m}} + {}^{i}P_{\mathrm{loss\_as\_c}}}{U_{\mathrm{m}}I_{\mathrm{m}}} \right]^2 + \left[ 1 - \frac{{}^{i}P_{\mathrm{loss\_in\_c}}}{P_{\mathrm{loss\_in\_m}}} \right]^2 + \left[ 1 - \frac{{}^{i}P_{\mathrm{loss\_ch\_c}}}{P_{\mathrm{loss\_ch\_m}}} \right]^2 \right\}^{\frac{1}{2}} \quad (2)
$$

As demonstrated in [3] on several experiments differing in the input power between approx. 5 and 25 kW, the value of $\delta_{\mathrm{tot1}}$ (2) has increased significantly in comparison to usual values of $\delta_{\mathrm{tot0}}$ and reached unacceptable levels, surprisingly under medium input powers mainly (the worst case: $U_{\mathrm{m}}I_{\mathrm{m}} = 18.4\,\mathrm{kW}$, $\delta_{\mathrm{tot1}} = 0.35$).

Deeper analysis of individual terms of (2) has clearly revealed the source of the discrepancy. While the relative error of voltage (i.e. the first fraction in (2)) was lower than 0.03, the second and third fractions, i.e. relative errors of the power losses of the input part and the anode channel, were several times higher and even of opposite sign to each other. Consequently, if only the total power loss was checked, this discrepancy remained hidden. Obviously, the way of evaluating the arc power loss in the model needs a revision.

In all the previous versions of the model the same procedure was used for estimating the arc's power loss. The power loss of the arc in each step in the computational mesh was computed as a portion of the electric input power using the power-loss coefficient $p_{\mathrm{loss}}$. This coefficient was determined from the integral measured values as follows

$$
{}^{i}p_{\mathrm{loss}} = \frac{P_{\mathrm{loss\_tot\_m}} - P_{\mathrm{loss\_cat\_m}} - {}^{(i-1)}P_{\mathrm{loss\_as\_c}}}{{}^{i}U_{\mathrm{A\_c}}(z_{\mathrm{L}})I_{\mathrm{m}}} \quad (3)
$$

In the $i^{\mathrm{th}}$ computational cycle, the measured total power loss $P_{\mathrm{loss\_tot\_m}}$ was decreased by the measured power loss of the cathode $P_{\mathrm{loss\_cat\_m}}$ and the computed power loss of the anode spot $P_{\mathrm{loss\_as\_c}}$, and divided by the computed arc input power $U_{\mathrm{A\_c}}(z_{\mathrm{L}})I_{\mathrm{m}}$. Then this coefficient was applied to determine the power loss of the arc in each step in the computational mesh, thus the same ratio between the arc's input power and its power loss was applied over the total length of the arc, in all the parts of the arc heater's anode channel. This simple approach evidently works well if the output parameters of the device are of main interest. Unfortunately, it fails if the internal distribution is studied in individual parts of the anode channel where significantly different conditions rule. Probably, it is especially the input part of the anode channel which differs from the others as the arc is yet to arise there and its radius and temperature change steeply.

Based on the above given observation and consideration, the computation of the arc's power loss has been modified. Previous experiments and calculations have shown that the arc power loss is due to arc radiation and the gas temperature near the channel wall is equal to the input temperature of cold gas. The experiments discussed here have been carried out with the arc burning in pure argon. The net emission coefficient of argon under normal pressure and in the temperature range up to 30 000 K has been computed by Dr. Petr Kloc [4] and is utilized for estimation of irradiated power from the arc as follows

$$
{}^{i}\Delta P_{\mathrm{loss\_A}}(z_j) = \frac{\pi^2}{2} \left\{ \epsilon \left[ {}^{i}T_{\mathrm{A}}(z_{j-1}), {}^{i}r_{\mathrm{A}}(z_{j-1}) \right] + \epsilon \left[ {}^{i}T_{\mathrm{A}}(z_j), {}^{i}r_{\mathrm{A}}(z_j) \right] \right\} \left[ {}^{i}r_{\mathrm{A}}(z_{j-1}) + {}^{i}r_{\mathrm{A}}(z_j) \right] \sqrt{\Delta z^2 + r_0^2 \left[ \left( \frac{z_j}{r_0} \right)^{\frac{1}{n_{\mathrm{r}}}} - \left( \frac{z_{j-1}}{r_0} \right)^{\frac{1}{n_{\mathrm{r}}}} \right]^2} \Delta z \quad (4)
$$

Here, ${}^{i}\Delta P_{\mathrm{loss\_A}}$ is the computed power loss of the arc in the $i^{\mathrm{th}}$ computational cycle and at the step between $z_j$ and $z_{j-1}$, $\epsilon$ is the net emission coefficient of argon for the given temperature and radius, $r_{\mathrm{A}}$ is the arc column radius, $r_0$ is the radius at the very beginning, at the cathode. Obviously, rather simple computation is applied to test the effect of using the net emission coefficient for calculation of the irradiated power. Averaged values of net emission coefficient are used and the power irradiated through the lateral surface of each elementary segment $\Delta z$ is taken to be absorbed by the channel wall. Even so the influence on the computed power loss of individual parts of the anode channel has been supposed to be substantial because the net emission coefficient exhibits significant dependence both on the radius and temperature. Summation of power loss increments (4) over the input part, the channel and the anode gives their computed power losses as demonstrated in the following section.

Furthermore, computations have shown that an achievable minimum of (2) is distinctly influenced also by the current density $j_0$ on the cathode. This parameter defines the radius $r_0$, and thus the development of the arc radius $r_{\mathrm{A}}$ along the axial coordinate $z$ [5]

$$
r_{\mathrm{A}}(z) = r_0[1 + (\frac{z}{r_0})^{\frac{1}{n_{\mathrm{r}}}}] \quad (5)
$$

Previously, $j_0 = 10^8\,\mathrm{A\,m^{-2}}$ was used, but now our further computations have indicated that several times higher values could lead to lower values of $\delta_{\mathrm{tot1}}$. Higher values of current density on the tungsten cathode are given e.g. in [6], [7] thus our observation does not contradict experimental results.

After the modifications explained above, such a set of three parameters $[n_r; j_0; T_{\mathrm{A}}(s)]$ has been sought for

during the computations, which is giving the minimum value of $\delta_{\mathrm{tot1}}$ (2). The modified procedure has been tested for the worst-case experimental results where the previous version has led to unacceptable differences.

## 3. Results and discussion

As shown in [3] and mentioned above, when the older version of the model has been used, the worst agreement between the measured and computed power losses of the input part and of the main part of the anode channel have been found for medium input power. In this section, the modified version of the model is intentionally tested for this worst-case example. In the following, a comparison of the dependences computed by the older version and the modified version of the model is given and discussed.

The analyzed experimental data have been measured on the arc heater whose geometry is defined by the following parameters: the anode channel radius $r = 8\,\mathrm{mm}$, the total anode channel length $z_{\mathrm{L}} = 109\,\mathrm{mm}$, the input part length $l_{\mathrm{in}} = 22\,\mathrm{mm}$, the anode channel length $l_{\mathrm{ch}} = 60\,\mathrm{mm}$, the grounded anode length $l_{\mathrm{an}} = 27\,\mathrm{mm}$. The arc has been blasted by the argon flow rate of $22.5\,\mathrm{g\,s^{-1}}$. The total measured voltage $U_{\mathrm{m}} = 113.4\,\mathrm{V}$, the arc current $I_{\mathrm{m}} = 162.3\,\mathrm{A}$, and the measured power losses of the anode channel's input part, the main part and of the grounded anode are 885.3 W, 1453.7 W and 1553.9 W, respectively.

Table 1 compares the obtained results of the older version of the model (the last row) and four best results obtained by the new version. Obviously, a significant improvement has been achieved comparing $\delta_{\mathrm{tot0}}$ (1) in the last row with arbitrary one of $\delta_{\mathrm{tot1}}$ (2) in the first four rows.

Mutual comparison of the results of the new version of the model in the first four rows shows almost negligible differences in the achieved $\delta_{\mathrm{tot1}}$. The final choice of the most suitable variant of them has been made with respect to the computed axial dependence of the arc temperature $T_{\mathrm{A}}(z)$ in the close vicinity of the beginning (Figure 1). The variant no. 3 [2.55; $2.67 \times 10^8\,\mathrm{Am^{-2}}$; 12700 K] exhibits the smoothest increase without oscillations. This variant is selected for the following discussion and comparison. Nevertheless, it is worth noting that the computed temperature dependences of all four variants differ only near the beginning and almost merge at about 4 mm from the beginning.

In the following figures, the results obtained by the older version of the model (var. no. 5 in Tab. 1) are denoted with the abbreviation pl (as obtained using the total power loss coefficient $p_{\mathrm{loss}}$) and plotted in dashed lines, while the results obtained by the new version of the model (var. no. 3 in Tab. 1) are denoted with the abbreviation nec (as obtained using the net emission coefficient) and plotted in solid lines.

The left side of Figure 2 shows the computed axial development of the arc temperature and radius.

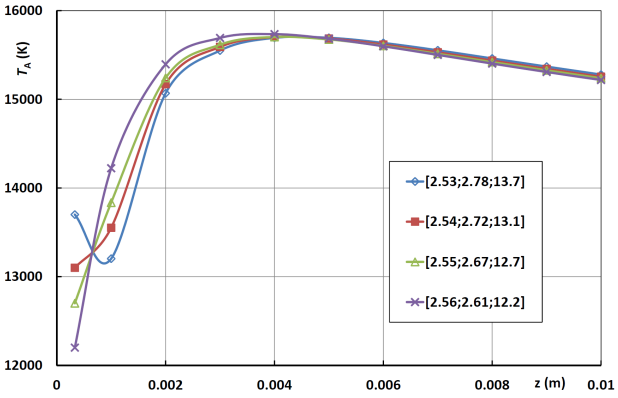


*Figure 1. Detailed comparison of the computed arc temperature axial dependence $T_{\mathrm{A}}(z)$ near the beginning of the anode channel, for 4 sets of $[n_{\mathrm{r}};\ j_0 \times 10^{-8};\ T_{\mathrm{A}}(s) \times 10^{-3}]$ near the lowest value of $\delta_{\mathrm{tot1}}$.*

Obviously,using the constant total power loss coefficient for all the parts of the arc suppresses the differences between individual parts and thus results in lower temperatures with rather flat axial dependence. On the contrary, the net emission coefficient, which is strongly dependent on radius and temperature, emphasizes the differences and thus results in distinctly higher temperatures with steeper axial dependence. Of course, with the radii, an opposite influence is observed: higher temperatures are accompanied with lower radii and the shape of the dependence $r_{\mathrm{A}}(z)$ is preserved as defined by (5). The results of the new version of the model meet our preliminary assumptions and also the expected behavior of the intensively blasted electric arc.

In the right side of Figure 2 axial dependences of the electric field intensity and the arc potential are given. The arc voltage computed by the new version of the model (var. no. 3 in Tab. 1) is higher than that obtained from the older version (var. no. 5 in Tab. 1). Unfortunately, as can be seen in Tab. 1, it is too high. The relative error of the arc voltage $\delta U$ for all the four variants (var. no. 1 to 4) is positive and significantly prevails the relative errors of the power losses of the anode channel's input and main parts. Mutual relation between voltage and power-loss relative errors is opposite with the model using the net emission coefficient compared to the model using the constant total power-loss coefficient. While the older version of the model reaches very good agreement between the computed and measured voltages and fails in power losses computation, the modified version achieves very good conformity in power losses but the relative error of voltage worsens. In all the four variants no. 1 to 4 the voltage relative error is almost 0.09, which is about five times worse than in var. no. 5, and represents almost the whole of $\delta_{\mathrm{tot1}}$. This issue will be further investigated to reveal its cause and to find an acceptable explanation.

| **Var.** No. | $n_\mathrm{r}$ (-) | $j_0 \times 10^{-8}$ (A m$^{-2}$) | $T_\mathrm{A}(s)$ (K) | $s$ (mm) | $T_\mathrm{A}(z_1)$ (K) | $\delta_\mathrm{in} \times 10^2$ (-) | $\delta_\mathrm{ch} \times 10^2$ (-) | $\delta_\mathrm{U} \times 10^2$ (-) | $\delta_\mathrm{tot} \times 10^2$ (-) | **loss** |
|---|---|---|---|---|---|---|---|---|---|---|
| 1 | 2.53 | 2.78 | 13 700 | 0.453 | 13 203 | −0.58 | −0.35 | 8.92 | 8.94 | nec |
| 2 | 2.54 | 2.72 | 13 100 | 0.404 | 13 552 | −0.67 | −0.58 | 8.92 | 8.96 | nec |
| 3 | 2.55 | 2.67 | 12 700 | 0.372 | 13 835 | −0.63 | −0.41 | 8.95 | 8.98 | nec |
| 4 | 2.56 | 2.61 | 12 200 | 0.332 | 14 223 | −0.30 | −0.81 | 8.98 | 9.02 | nec |
| 5 | 2.76 | 1.00 | 9 400 | 0.346 | 10 111 | 23.86 | −17.72 | −1.86 | 34.83 | pl |

*Table 1. Comparison of several selected variants.*

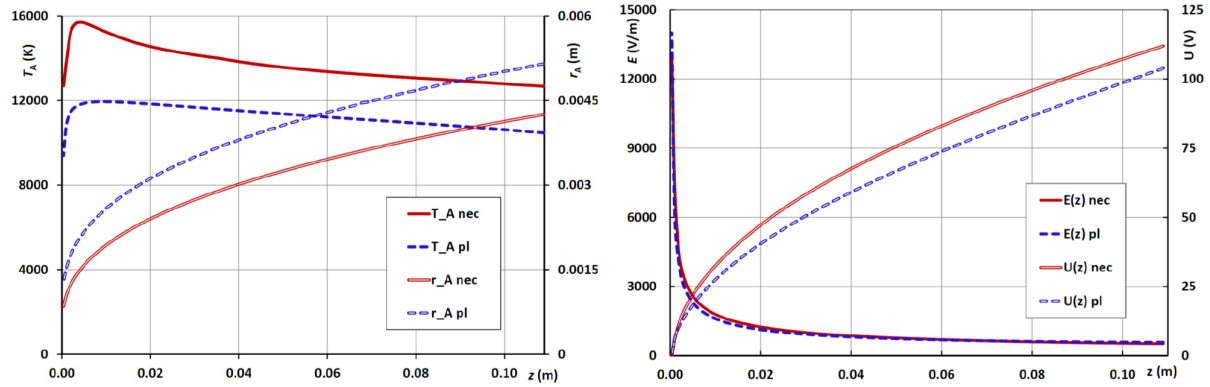


*Figure 2. Comparison of axial dependences of the arc temperature $T_\mathrm{A}(z)$ and the arc radius $r_\mathrm{A}(z)$ (left) and of the electric field intensity $E(z)$ and the arc potential $U(z)$ (right) computed by the arc model using two different methods of computation of the arc power loss: nec - net emission coefficient of argon (var. no. 3), pl - constant power loss ratio (var. no. 5).*

## 4. Conclusions and further work

The paper introduces the modified version of the simplified model of the intensively blasted electric arc burning in argon inside the cylindrical anode channel of the arc heater. As previous versions failed in computation of power losses of individual parts of the anode channel, the new method of estimation the arc's power loss has been applied using the theoretically calculated values of net emission coefficient of argon. Simultaneously, also the initial current density has been included into the set of state variables $[n_\mathrm{r}; j_0; T_\mathrm{A}(s)]$ instead of being kept constant. The modified model has been tested on the experimental data which previously have exhibited the worst agreement of computed and measured values. Significant improvement has been achieved in comparison with the results of the older version of the model. The obtained dependences meet the preliminary expectations about the behavior of intensively blasted electric arc. Altogether with a significant decrease of relative errors of power losses, the relative error of voltage increased several times in the new model. The explanation could lie in still neglected phenomena and certainly will be sought for during further tests of the modified model with other sets of experimental data.

### Acknowledgements

Authors gratefully acknowledge financial support from the Ministry of Education, Youth and Sports of the Czech Republic under NPU I programme (project No. LO1210) and from the Czech Science Foundation under project No. GA 15-14829S. The authors thank Dr. Petr Kloc for computation of net emission coefficient of argon.

### References

[1] J. Senk, I. Jakubova, and I. Laznickova. Analysis of intensively blasted electric arc burning in the arc heater's anode channel. *Acta Polytechnica*, 56(5):395–401, 2016. doi:10.14311/AP.2016.56.0395.

[2] J. Senk, I. Jakubova, and I. Laznickova. Remarks on the design of high-temperature devices with electric arc. In *Proc. of the 15th Internat. Sci. Conf. Electric Power Engineering*. FEEC Brno University of Technology, 2014.

[3] J. Senk, I. Laznickova, and I. Jakubova. Power loss distribution along the arc heater with intensively blasted electric arc. In *Proc. of the 18th Internat. Sci. Conf. Electric Power Engineering*. To be published, 2017.

[4] P. Kloc, V. Aubrecht, M. Bartlova, and O. Coufal. Radiation transfer in air and air-Cu plasmas for two temperature profiles. *J Phys D: Appl Phys*, 48(5):1–13, 2015. doi:10.1088/0022-3727/48/5/055208.

[5] Herman Schlichting. *Grenzschicht Theorie*. Verlag G. Braun, Karlsruhe, Germany, 1965.

[6] A. Bauer. Zur theorie des kathodenfalls in lichtbogen. *Z. Physik*, 138:35–55, 1954. doi:10.1007/BF01365533.

[7] A. A. Belevtsev et al. Experimental study of the near-electrode plasma-tungsten cathode system in high-current athmospheric-pressure nitrogen arcs. *High Temperature*, 51(5):583–593, 2013. doi:10.1134/S0018151X13050027.